Increased valency improves inhibitory activity of peptides targeting proprotein convertase subtilisin/kexin type 9 (PCSK9)

Mr. Benjamin J. Tombling[1], Dr. Carmen Lammi[2], Dr. Carlotta Bollati[2], Prof. Anna Anoldi[2], Prof. David, J. Craik[1], Dr. Conan K. Wang[1]*

[1] Institute for Molecular Bioscience, Australian Research Council Centre of Excellence for Innovations in Peptide and Protein Science, The University of Queensland, Brisbane, Qld, 4072, Australia

[2] Dipartimento di Scienze Farmaceutiche, Università degli Studi di Milano, Via L. Mangiagalli 25, 20133 Milan, Italy

* Corresponding author: c.wang@imb.uq.edu.au

Twitter handles: @BTombling @TheCraikGroup @ARC_CIPPS @IMBatUQ @researcherconan

Abstract

Proprotein convertase subtilisin/kexin type 9 (PCSK9) is a clinically validated target for treating hypercholesterolemia. Peptide-based PCSK9 inhibitors have attracted pharmaceutical interest, but the effect of multivalency on bioactivity is poorly understood. Here we designed bivalent and tetravalent dendrimers, decorated with the PCSK9 inhibitory peptides Pep2-8[RRG] or P9-38, to study relationships between peptide binding affinity, peptide valency, and PCSK9 inhibition. Increased valency resulted in improved PCSK9 inhibition for both peptides, with activity improvements of up to 100-fold achieved for the P9-38-decorated dendrimers compared to monomeric P9-38 in *in vitro* competition binding assays. Furthermore, the P9-38-decorated dendrimers showed improved potency at restoring functional low-density lipoprotein (LDL) receptor levels and internalizing LDL in the presence of PCSK9, demonstrating significant cell-based activity at picomolar concentrations. This study demonstrates the potential of increasing valency as a strategy for increasing the efficacy of peptide-based PCSK9 therapeutics.

INTRODUCTION

Familial hypercholesterolemia (FH) is the most common inherited metabolic disorder, affecting an estimated 1 in 200 people globally,[1] and is a major cause of premature onset of cardiovascular disease (CVD).[2-4] FH causes autosomal dominant mutations in the protein machinery responsible for cholesterol metabolism, which impairs low-density lipoprotein (LDL)-cholesterol (LDL-C) clearance from plasma. Proprotein convertase subtilisin/kexin type 9 (PCSK9) was discovered to be a major locus associated with FH,[5] as it primarily regulates LDL receptor (LDLR) levels on hepatocyte surfaces.[6-9] LDLR is responsible for removing LDL-C from plasma using a receptor-mediated endocytosis pathway that ends up in LDLR recycling back to the cell surface.[10] Serum PCSK9 impairs LDL-C uptake by binding to LDLR on cell surfaces and chaperoning the internalized PCSK9:LDLR complex to the lysosome for degradation, thereby preventing LDLR recycling.[11] Based on its major role in cholesterol metabolism, PCSK9 has attracted wide interest as a therapeutic target for treating hypercholesterolemia.

Many approaches are being explored for targeting PCSK9 inhibition[12-14] and the most successful and validated approach involves preventing PCSK9 binding to the extracellularly located epidermal growth factor domain A (EGF-A) of the LDLR. PCSK9 forms a flat ~500 Å binding interface with EGF-A.[15-17] Two approved monoclonal antibodies, that inhibit PCSK9 binding to LDLR, significantly reduce LDL-C levels by ~50–60% and reduce the occurrence of CVD in patients that do not respond sufficiently to statin medication.[18-20] However, the clinical use of these antibodies is limited by their high cost.[21-22] Given the ability of peptides to block protein–protein interactions (PPIs) with high specificity,[23-24] peptides have gained attention as promising antagonists of PCSK9 with improved cost-effectiveness

compared to monoclonal antibodies.[25-31] For example, the phage-derived peptide Pep2-8 selectively competes with EGF-A for binding to PCSK9,[26] and Pep2-8 has subsequently been used as a lead to design next-generation peptide antagonists with improved activity.[28-29, 32] We recently optimized Pep2-8 with a bioactive cyclization linker (a linker designed with functional amino acids that enable specific binding to PCSK9 whilst also structurally achieving a cyclic peptide structure) to identify the engineered cyclic peptide P9-38.[33] P9-38 demonstrated ~100-fold improved affinity for PCSK9, compared to Pep2-8, which translated to significantly increased potency for restoring LDLR function. Although PCSK9-targeted peptides have shown promising inhibition activities, strategies that easily enhance their activities would be beneficial to boost their therapeutic potential.

Dendrimers have attracted interest as scaffolds to display multiple copies of peptides.[34] Dendrimers are well-characterized branched polyvalent structures that can be functionalized with a high density of bioactive epitopes covalently attached to their surface.[35] Traditionally, dendrimers have been broadly used for drug delivery and solubility enhancer bioapplications.[36-37] Furthermore, dendrimers functionalized with multiple copies of a therapeutic peptide have shown improved activity over their monomeric counterparts, in part due to enforcing a higher local effective concentration of peptide binding motifs positioned near the desired target binding site (see Figure 1). For example, peptide-decorated dendrimers have successfully targeted immune responses,[38-40] viral infections,[41] nicotinic acetylcholine receptors,[42] and G protein-coupled receptors.[43-44] Despite these examples, the use of peptide-decorated dendrimers to target disease-related PPIs, which are now recognized as a major class of druggable targets,[45-46] has been underexplored. So far, no multimeric peptides that target the PCSK9:LDLR interaction have been investigated.

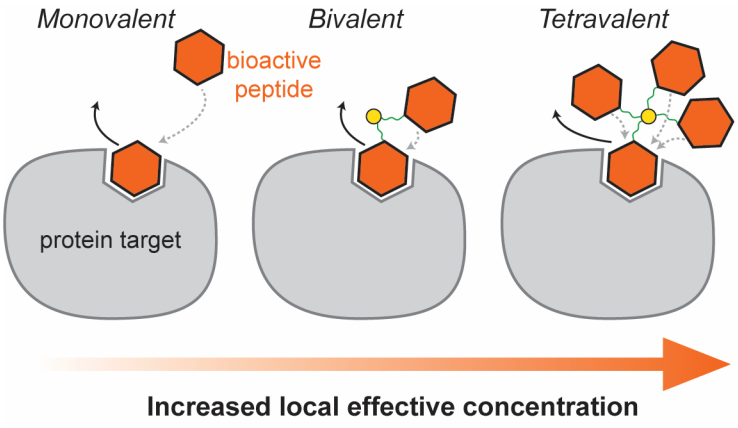

Figure 1. Concept of designing homomultivalent systems to improve the therapeutic activity of bioactive peptides. Dendrimers are an example of a polyvalent scaffold (yellow and green) that can be decorated with equivalent bioactive peptide pharmacophores (orange hexagons), resulting in an increased local effective concentration of bioactive peptides surrounding the desired protein target binding site (gray).

Here we aimed to determine whether increased peptide valency have improved PCSK9 inhibition activity. Using the PCSK9 antagonists Pep2-8[RRG] and P9-38,[33] we synthesized a panel of bivalent and tetravalent functionalized dendrimers that inhibited PCSK9 with up to ~100-fold improved activity over the monomeric peptides and restored LDLR function at sub-nanomolar concentrations in cell-based functional assays.

RESULTS

Synthesis of peptide-decorated dendrimers

Previous studies have shown that up to four copies of a ligand are required to reach a plateau in activity.[42, 44, 47] Therefore, we focussed our efforts towards designing and synthesizing bivalent and tetravalent peptide decorated dendrimers. First, the 2-mer and 4-mer azido-PEGylated-Lys dendron scaffolds, DS-2 and DS-4, were chemically synthesized by stepwise

Fmoc solid-phase peptide synthesis (Scheme S1A, Supporting Information). A Gly-Arg-Arg-Lys-Trp inner core linker was incorporated to aid with electrospray ionization mass spectrometry (ESI-MS) detection and to allow UV quantification at 280 nm.[44] PEGylated branches (specifically PEG_{10}) extending from the dendron core were used to provide a sufficient spacer segment to limit the possibility of steric hindrance of the conjugated peptides and to aid in aqueous solubility. The branches of the dendrimer scaffolds were capped with azido functional groups to allow chemoselective targeting using copper(I)-catalyzed alkyne-azide cycloaddition (CuAAC) click chemistry.[48]

The recently reported PCSK9-targeting peptide inhibitors, Pep2-8[RRG] (containing the -RRG C-terminus extension to aid aqueous solubility) and P9-38,[26, 33] were chosen as bioactive epitopes to functionalize the dendrimers. These peptides were selected because the monomers have ~100-fold difference in affinities for PCSK9, allowing us to explore the correlation between monomer affinity and valency on activity. Alkyne-functionalized analogues of Pep2-8[RRG] and P9-38, where the N-terminus of each peptide was labeled with an alkyne moiety, were synthesized and separately conjugated to the azido-dendron scaffolds (Scheme S1B, Supporting Information). We used $CuSO_4$, with sodium ascorbate as the reductant along with tris(benzyltriazolylmethyl)amine (THPTA) as a chelating ligand. To push the reaction towards complete coupling, four-fold and eight-fold excesses of alkyne-peptides were incubated with DS-2 and DS-4, respectively. The formation of the desired bivalent and tetravalent Pep2-8[RRG]- and P9-38-decorated dendrimers (see Figure 2), was confirmed by ESI-MS (Table S1, Supporting Information).

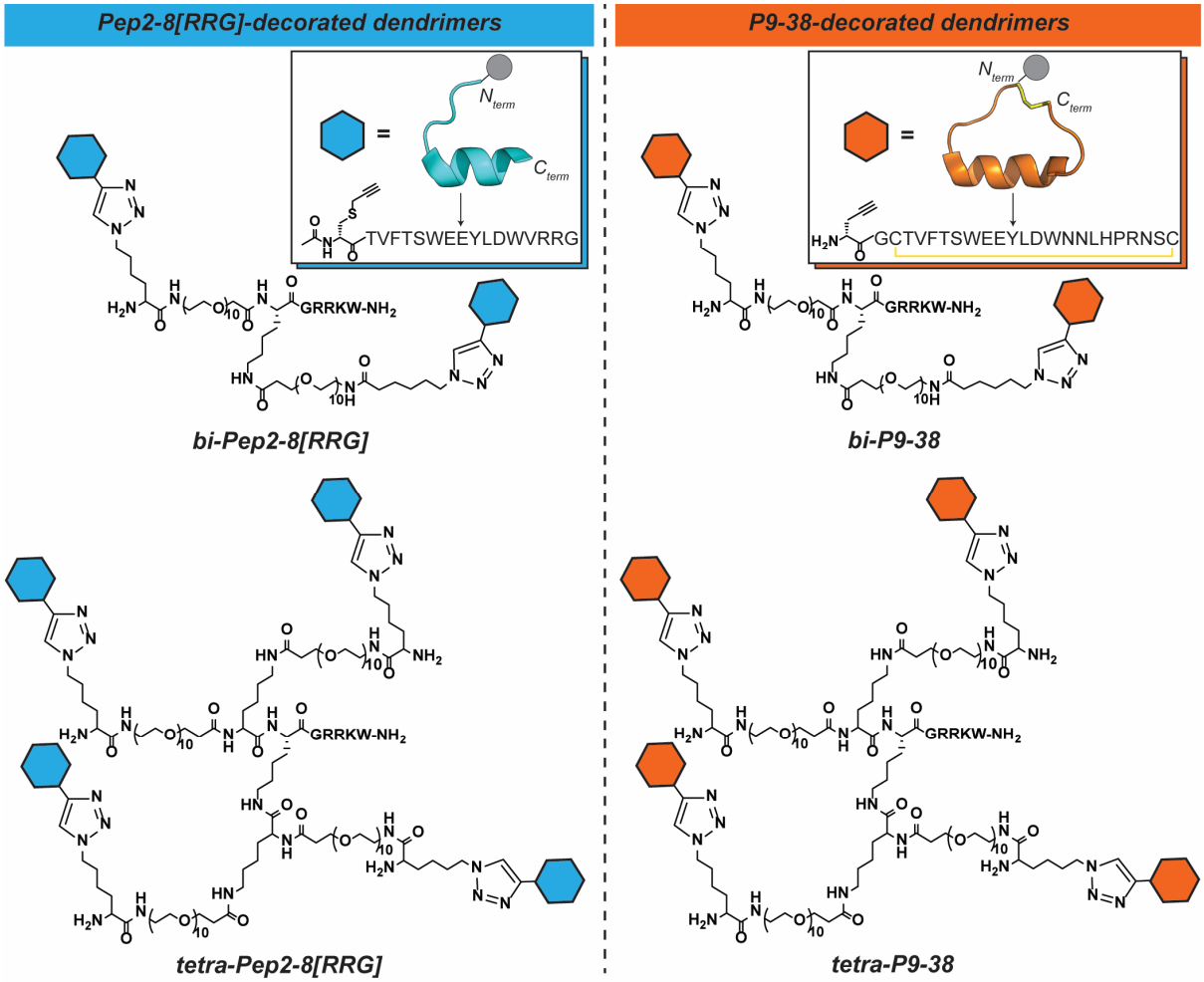

Figure 2. Bivalent and tetravalent Pep2-8[RRG]- and P9-38-decorated dendrimers designed and synthesized in this study. Branched structures were composed of a poly-Lys core framework with PEG_{10} linkers that were capped with azido-functional groups. A Gly-Arg-Arg-Lys-Trp inner core peptide linker was used to both aid with ESI-MS characterization and to allow accurate UV quantification at 280 nm. Analogues of the PCSK9-targeting peptides were designed with alkyne-functional groups at the N-terminus. Box inserts show the peptide bioactive structures, peptide sequences and site of alkyne-functionalization. The azido-dendrimer scaffolds were conjugated to the alkyne-peptide moieties using a standard copper(I)-catalyzed alkyne-azide cycloaddition (CuAAC) approach.

Structural characterization of peptide-decorated dendrimers

In addition to using mass analysis for characterization of the dendrimer analogues, we also performed structural characterization. First, we analyzed Pep2-8[RRG] peptide-decorated dendrimers using nuclear magnetic resonance (NMR) spectroscopy. Interestingly, two-dimensional TOCSY spectra of both bi-Pep2-8[RRG] and tetra-Pep2-8[RRG] showed the same

number of spin systems as monomeric Pep2-8[RRG]. Although this result does not provide validation of the number of copies attached to the dendrimer scaffold, it does show that each copy of Pep2-8 on the dendrimer scaffolds shared the same conformation. Hα secondary NMR chemical shifts of both bi-Pep2-8[RRG] and tetra-Pep2-8[RRG] were essentially identical to monomeric Pep2-8[RRG] (Figure 3), showing all dendrimer-attached copies of Pep2-8[RRG] adopt the parent conformation. Additionally, the negative secondary shifts indicate retention of the helical structure. CD spectroscopy confirmed helical structures for Pep2-8[RRG] and bi-Pep2-8[RRG] as indicated by minima in the spectra at 206 nm and 229 nm, which were not present for the non-decorated dendrimer scaffold DS-2 (Figure S1, Supporting Information). Together, these results confirmed the dendrimer scaffolds did not affect the conformation of the attached Pep2-8[RRG] peptide. This was expected because the conjugation site was specifically chosen to be distal to the helical pharmacophore of the peptide as not to affect peptide structure.

The P9-38-decorated dendrimers displayed poor aqueous solubility and, therefore, analysis of the Hα secondary NMR chemical shifts was unable to be performed. However, both Pep2-8[RRG] and P9-38 contain common bioactive sequence and active 3D structures for their binding pharmacophores (see Figure 2),[26, 33] and both are attached to their dendrimer scaffolds via their N-termini. Therefore, based on the similarity between Pep2-8[RRG] and P9-38, and results on Pep2-8[RRG] dendrimers, we suggest that P9-38 conformation would not be affected upon dendrimer conjugation. We conclude that the structural data provide support for the mass analysis demonstrating the desired dendrimer analogues were correctly synthesized.

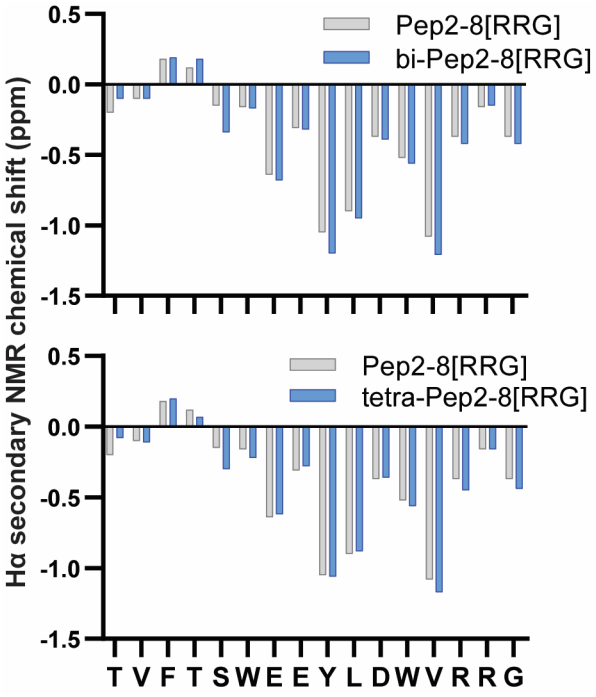

Figure 3. Structural characterization of Pep2-8-decorated dendrimers. Hα secondary NMR chemical shifts for Pep2-8[RRG] compared to bi-Pep2-8[RRG] (top panel) and Pep2-8[RRG] compared to tetra-Pep2-8[RRG] (bottom panel). NMR experiments were recorded in H_2O/D_2O (9:1 v/v) solution. Hα secondary NMR chemical shifts for the P9-38-decorated dendrimers could not be compared due to solubility issues.

Peptide-decorated dendrimers have improved inhibition of PCSK9 *in vitro*

The effects of peptide valency on PCSK9 inhibition were assessed using a recently described *in vitro* competition binding assay.[33] The Pep2-8[RRG]-decorated dendrimers had improved ability to inhibit PCSK9 binding to an analogue of its native protein binding partner (tEGF-A[HA]) compared to monovalent Pep2-8[RRG] (Figure 4A). Specifically, bi-Pep2-8[RRG] had an IC_{50} of 0.23 ± 0.34 μM, which was ~5-fold more potent than Pep2-8[RRG].[33] The activity of tetra-Pep2-8[RRG] was increased compared to bi-Pep2-8[RRG], however poor solubility made it difficult to accurately determine activity values. Nonetheless, it appeared there was a trend between increased valency and improved activity.

The benefits of multivalency were more apparent for the P9-38-decorated dendrimers, as both the bivalent and tetravalent compounds showed improved inhibition compared to monovalent P9-38. Bi-P9-38 and tetra-P9-38 inhibited PCSK9 binding to tEGF-A[HA] with IC_{50} values of 0.33 ± 0.29 nM and 0.18 ± 0.14 nM, respectively (Figure 4B). This corresponds to a ~60–100-fold improvement in activity compared to monomeric P9-38,[33] demonstrating remarkable sub nanomolar activity for the P9-38-decorated dendrimers. Interestingly, little activity was gained by increasing the valency from bivalent to tetravalent, suggesting bivalency was enough to reach the binding efficiency threshold that could be achieved based on the parent P9-38 activity. The dendrimer scaffold DS-2 showed no ability to inhibit the PCSK9:tEGF-A[HA] interaction at 20 μM (Figure S3, Supporting Information), confirming that the enhanced activity of the peptide-decorated dendrimers was solely due to the peptide binding epitopes.

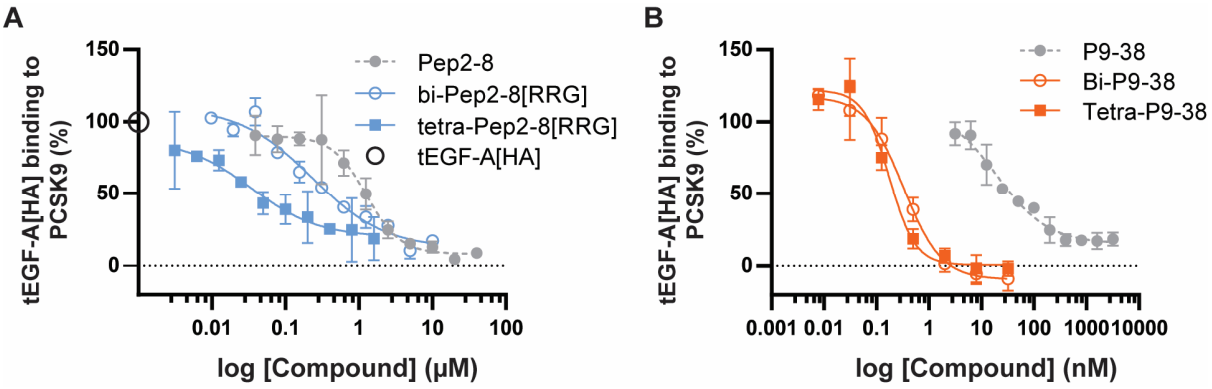

Figure 4. Peptide-decorated dendrimers inhibit PCSK9 binding to tEGF-A[HA]. (A) Pep2-8[RRG]-decorated dendrimers and (B) P9-38-decorated dendrimers have improved PCSK9 inhibition compared to their parent monomeric peptides. The activity for Pep2-8[RRG] and P9-38 has been previously reported.[33] 100% binding represents tEGF-A[HA] binding to PCSK9 in the presence of no inhibitor, as indicated by the open circle in panel A. Results are normalized to this value. Data are the average ± s.d from three independent experiments.

To understand the mechanism driving improved inhibitory activity due to multivalency, we analyzed the binding affinity of the bivalent peptide-decorated dendrimers to PCSK9 using

surface plasmon resonance (SPR). The SPR sensorgrams for Pep2-8[RRG] and bi-Pep2-8[RRG] showed similar curvature (Figure S4, Supporting Information), indicating no major changes in the association and dissociation kinetic binding rate constants. This translated to equilibrium dissociation constants (K_D) of 0.84 ± 0.06 μM and 0.40 ± 0.01 μM for Pep2-8[RRG] and bi-Pep2-8[RRG], respectively (Figure 5A). The ~2-fold higher PCSK9 affinity of bi-Pep2-8[RRG] agreed with the competitive binding data and confirmed that only modest activity improvements were observed for Pep2-8[RRG] bivalency.

P9-38 bivalency gave a clearer binding difference. The sensorgrams displayed in Figure 5B show the normalized binding of P9-38 and bi-P9-38 (both injected at 50 nM) to PCSK9 and indicate no differences in the association rate of P9-38 and bi-P9-38 to PCSK9. However, bi-P9-38 had a dramatically slower dissociation rate than P9-38. Approximately 70% of bi-P9-38 remained bound to PCSK9 after 5 min of a constant flow of running buffer over the immobilized PCSK9 surface whereas, at the same timepoint, monomeric P9-38 was fully dissociated (Figure 5C). Furthermore, the increased binding strength of bi-P9-38 retains selectivity for the desired PCSK9 binding site as monomeric P9-38 was unable to efficiently bind to PCSK9 after treatment with bi-P9-38 (Figure S5, Supporting Information). Due to poor curve fitting, K_D constants could not be accurately determined for bi-P9-38. However, the binding kinetic parameters obtained for the single concentration (50 nM) of P9-38 were in agreement with our previous PCSK9 affinity results (K_D of 8.4 ± 0.35 nM and 7.7 ± 1.4 nM, respectively),[33] indicating that the single concentration sensorgrams were an accurate portrayal of affinity. The important conclusion from the SPR data is that it supported the competition binding assays in showing that the multivalent compounds have an improved ability to inhibit PCSK9, compared to their respective monomers, with the most notable improvements in activity observed for the P9-38-decorated dendrimers.

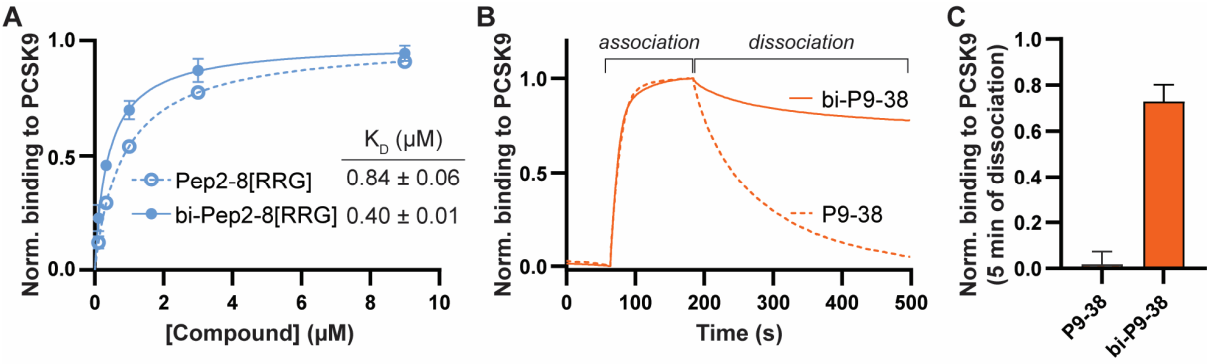

Figure 5. *In vitro* binding of peptide-decorated dendrimers to PCSK9. (A) Steady state binding affinity of Pep2-8[RRG] and bi-Pep2-8[RRG] binding to PCSK9. SPR sensorgrams were analyzed by taking the response (RU) for each peptide concentration tested and normalizing the signal to the experimentally determined RU max for each peptide. The K_D values are the average ± s.d. (B) Overlay of the SPR sensorgrams for P9-38 and bi-P9-38 binding to PCSK9. Both compounds were tested at 50 nM. Sensorgrams are normalized to the RU max for each peptide. The association and dissociation phases are characterized by the time when peptide analyte flowed over the PCSK9 immobilized surface is replaced by reaction buffer. (C) The amount of P9-38 and bi-P9-38 that remained bound to PCSK9 after 5 min of reaction buffer flowed over the immobilized surface. Binding levels are normalized to the maximum RU response determined during the association phase. Results are the average ± s.d of two independent experiments.

P9-38-decorated dendrimers restore LDLR function

The enhanced *in vitro* activity and affinity of the P9-38-based dendrimers suggested they would display the greatest functional activity; therefore, we investigated their ability to inhibit PCSK9 in model liver cell (HepG2)-based assays. Bi-P9-38 and tetra-P9-38 were shown to be non-toxic to HepG2 cells (tested up to 100 nM), excluding any cytotoxic effects attributed to the PEGylated dendrimer scaffolds (Figure S6, Supporting Information).

The ability of bi-P9-38 and tetra-P9-38 to inhibit PCSK9 and thereby restore the number of LDLRs on HepG2 cells was investigated. PCSK9 (4 μg/mL) reduced the surface levels of LDLR by 45.6 ± 4.9%. As shown in Figure 6A, bi-P9-38 fully restored surface LDLR levels

at 10 nM (100.2 ± 6.1%) and showed significant activity at low picomolar concentrations (74.5 ± 6.0% and 81.3 ± 6.1% at 10 and 100 pM, respectively). Tetra-P9-38 showed a similar ability to increase LDLR levels in the presence of PCSK9, fully restoring LDLR levels at 10 nM (102.7 ± 16.9%) and induced a considerable increase in LDLR levels at 10 pM (67.8 ± 9.9%). In contrast, P9-38 was only able to restore LDLR levels to ~88% when administered at 10 nM, highlighting the improved functional activity of the P9-38-decorated dendrimers.

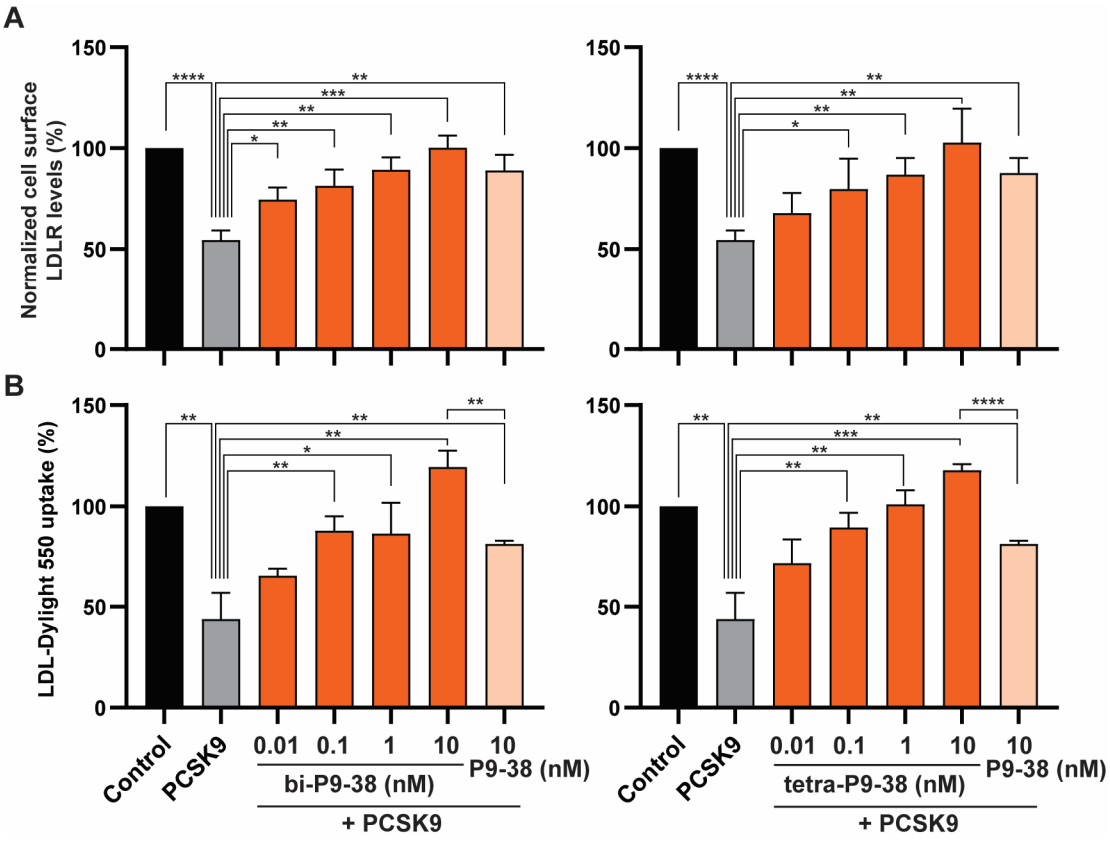

Figure 6. P9-38-decorated dendrimers have an improved ability to restore LDLR function compared to P9-38. Bi-P9-38 data and tetra-P9-38 data are shown in the left and right panels, respectively. P9-38 (10 nM) is used as a comparison for all experiments. (A) Bi-P9-38 and tetra-P9-38 restores LDLR surface levels on HepG2 cells in the presence of PCSK9. * for $p < 0.05$ and ** for $p < 0.01$. (B) Uptake efficiency of fluorescently labeled LDL by HepG2 cells induced by PCSK9 is improved by bi-P9-38 and tetra-P9-38. HepG2 cells with no peptide or PCSK9 treatment were used as a control. * for $p < 0.05$, ** for $p < 0.01$, *** for $p < 0.001$, and **** for $p < 0.0001$. Results are average ± s.d of three independent experiments, each performed with three replicates.

PCSK9 impairs the ability of the LDLR to efficiently transport LDL for intracellular degradation. Therefore, the functional activity of the P9-38-decorated dendrimers was further assessed by monitoring their ability to increase the uptake of fluorescent LDL in the presence of PCSK9 (Figure 6B). As expected, HepG2 cells treated with PCSK9 alone had reduced ability to uptake LDL by 56.2 ± 13.1% to compared to untreated cells. However, when bi-P9-38 and tetra-P9-38 were incubated with PCSK9 before cell treatment, LDL uptake was fully restored at 10 nM (119.4 ± 8.2% and 117.8 ± 3.1%, respectively). By comparison, 10 nM of P9-38 showed significantly weaker efficacy and only improved LDL internalization to 81.4 ± 1.7%, which was a similar level of efficacy achieved by 100 pM of bi-P9-38 and tetra-P9-38 (87.9 ± 7.2% and 89.5 ± 7.2%, respectively). These results comprehensively indicate that multivalent P9-38-decorated dendrimers have up to ~100-fold improved biological activity towards restoring LDLR function over monomeric P9-38.

DISCUSSION

In this study we designed multivalent peptide-decorated dendrimers that have improved PCSK9 inhibition. Site-selective chemical synthesis strategies were used to yield bivalent and tetravalent dendrimer scaffolds functionalized with the peptide PCSK9 antagonists Pep2-8[RRG] and P9-38. Competition assays confirmed that the multivalent compounds had improved inhibition, with the bivalent and tetravalent P9-38-decorated dendrimers showing ~60- and ~100-fold improved ability to inhibit the PCSK9:EGF-A interaction compared to monomeric P9-38. Furthermore, the P9-38-decorated dendrimers showed improved potency and efficacy, compared to P9-38, at inhibiting PCSK9 in cell-based assays and restoring LDLR function at picomolar concentrations. Altogether, the P9-38-decorated dendrimers are two of

the most active peptide-based inhibitors of PCSK9 reported to date and demonstrate the potential of multivalent inhibitors as cholesterol-lowering therapeutics.

In addition to showing that multivalency triggers an increase in functional activity, our results revealed an interesting correlation between affinity, valency, and activity. Given that P9-38 has ~100-fold stronger affinity for PCSK9 compared to Pep2-8[RRG],[33] our results suggest that higher affinity pharmacophores require fewer copies to achieve optimal binding compared to lower affinity ligands, however, we appreciate that increased valency beyond that reported in here may be required to confirm this observation. For example, bivalent ligands of Pep2-8[RRG] had ~5-fold improved activity and similar binding kinetics compared to monomeric Pep2-8[RRG], whereas bi-P9-38 had an enhanced ~60-fold improvement in activity and a dramatically slower binding dissociation rate than monomeric P9-38. Remarkably, this corresponds to each P9-38 ligand in bi-P9-38 being ~30-fold more active than monomeric P9-38. In addition, increasing the valency to tetrameric compounds appeared to improve the activity of Pep2-8[RRG]-based ligands with greater effect compared to P9-38-based ligands. The ability to decorate multivalent scaffolds with a low copy of bioactive ligands to achieve optimal binding is advantageous from a drug design perspective as it simplifies chemical synthesis strategies and reduces the risk of undesired immunogenicity.

The increased activity of the peptide ligands in the multivalent dendrimers is probably a result of the increased local effective concentration of ligand surrounding the PCSK9 target site which increases the probability of ligand interaction compared to a diffusion-related mechanism associated with monomeric ligands. In general, our results highlighting the benefits of using multivalency to target PCSK9 agree with a reported bivalent llama-human chimera

antibody.[49] However, in the case of the bivalent P9-38-decorated dendrimer, we achieved a 5-fold greater improvement in activity when applying multivalency. Overall, this work is the first to demonstrate the therapeutic potential of homomultivalent peptide-based PCSK9 inhibitors, and the results show the benefits of broadly implementing peptide-decorated dendrimers as a strategy for targeting validated disease-related PPIs.

The branched structure of dendrimers can be exploited to achieve scaffold multifunctionality. Several distinct pharmacophores can be attached to the dendrimer surface to design heterogenic multivalent compounds that display synergistic polypharmacology. For example, PCSK9 inhibitors and GLP-1 analogues have been investigated as a co-treatment for Type 2 diabetes,[50-51] and PCSK9 inhibitors have recently been shown to enhance the efficacy of immune checkpoint therapeutics such as PD-1 inhibitors for treating cancer.[52] Dendrimers can also be designed to address other limitations of peptides such as short circulating half-lives *in vivo*. Co-functionalizing the dendrimers with epitopes that confer serum protein binding, such as albumin-binding tags,[53-54] will improve the pharmacokinetics and decrease the therapeutic dosing frequency.

In conclusion, we have successfully demonstrated that homomeric multivalency is a promising approach for inhibiting PCSK9-mediated degradation of LDLR. By functionalizing dendrimer scaffolds with the PCSK9-targeting peptides Pep2-8 and P9-38, we achieved up to ~100-fold improved activity and efficacy over parent monomeric peptides. As a result, the P9-38-decorated dendrimers represent a new peptide-based drug lead for treating hypercholesterolemia. The ease of scaffold functionalization further enhances the

attractiveness of using dendrimers to target PCSK9 and adds to the therapeutic potential of multivalent peptide inhibitors to be broadly exploited in peptide drug design.

SUPPORTING INFORMATION

Experimental details, RP-HPLC and ESI-MS characterization of peptides and peptide-decorated dendrimers, complimentary *in vitro* binding assay data, cell viability, CD and NMR structural data.

ACKNOWLEDGEMENTS

This work was supported by a grant from the National Health and Medical Research Council (APP1107403). DJC is an Australian Research Council Laureate Fellow (FL150100146) and work in his lab is supported by access to the facilities of the Australian Research Council Center of Excellence for Innovations in Peptide and Protein Science (CE200100012).

KEYWORDS

cell-based activity, drug design, inhibitors, PCSK9, peptide-decorated dendrimers

REFERENCES

[1] S. Singh, V. Bittner, *Curr. Atheroscler. Rep.* **2015**, *17*, 3.

[2] S. S. Gidding, M. A. Champagne, S. D. d. Ferranti, J. Defesche, M. K. Ito, J. W. Knowles, B. McCrindle, F. Raal, D. Rader, R. D. Santos, M. Lopes-Virella, G. F. Watts, A. S. Wierzbicki, *Circulation* **2015**, *132*, 2167-2192.

[3] J. L. Goldstein, H. H. Hobbs, M. S. Brown in *The Online Metabolic and Molecular Bases of Inherited Disease* (Eds.: A. L. Beaudet, B. Vogelstein, K. W. Kinzler, S. E. Antonarakis, A. Ballabio, K. M. Gibson, G. Mitchell), The McGraw-Hill Companies, Inc., New York, NY, **2014**.

[4] H. H. Hobbs, M. S. Brown, J. L. Goldstein, *Hum. Mutat.* **1992**, *1*, 445-466.

[5] M. Abifadel, M. Varret, J.-P. Rabès, D. Allard, K. Ouguerram, M. Devillers, C. Cruaud, S. Benjannet, L. Wickham, D. Erlich, A. Derré, L. Villéger, M. Farnier, I. Beucler, E. Bruckert, J. Chambaz, B. Chanu, J.-M. Lecerf, G. Luc, P. Moulin, J. Weissenbach, A. Prat, M. Krempf, C. Junien, N. G. Seidah, C. Boileau, *Nat. Genet.* **2003**, *34*, 154.

[6] S. W. Park, Y.-A. Moon, J. D. Horton, *J. Biol. Chem.* **2004**, *279*, 50630-50638.

[7] K. N. Maxwell, J. L. Breslow, **2004**, *101*, 7100-7105.

[8] S. Benjannet, D. Rhainds, R. Essalmani, J. Mayne, L. Wickham, W. Jin, M.-C. Asselin, J. Hamelin, M. Varret, D. Allard, M. Trillard, M. Abifadel, A. Tebon, A. D. Attie, D. J. Rader, C. Boileau, L. Brissette, M. Chrétien, A. Prat, N. G. Seidah, *J. Biol. Chem.* **2004**, *279*, 48865-48875.

[9] T. A. Lagace, D. E. Curtis, R. Garuti, M. C. McNutt, S. W. Park, H. B. Prather, N. N. Anderson, Y. K. Ho, R. E. Hammer, J. D. Horton, *J. Clin. Invest.* **2006**, *116*, 2995-3005.

[10] J. L. Goldstein, M. S. Brown, *Arterioscler. Thromb. Vasc. Biol.* **2009**, *29*, 431-438.

[11] A. S. Peterson, L. G. Fong, S. G. Young, *J. Lipid Res.* **2008**, *49*, 1152-1156.

[12] K. K. Ray, R. S. Wright, D. Kallend, W. Koenig, L. A. Leiter, F. J. Raal, J. A. Bisch, T. Richardson, M. Jaros, P. L. J. Wijngaard, J. J. P. Kastelein, *N. Engl. J. Med.* **2020**, *382*, 1507-1519.

[13] Y. Pan, Y. Zhou, H. Wu, X. Chen, X. Hu, H. Zhang, Z. Zhou, Z. Qiu, Y. Liao, *Sci. Rep.* **2017**, *7*, 12534.

[14] P. I. Thakore, J. B. Kwon, C. E. Nelson, D. C. Rouse, M. P. Gemberling, M. L. Oliver, C. A. Gersbach, *Nat. Commun.* **2018**, *9*, 1674.

[15] D.-W. Zhang, T. A. Lagace, R. Garuti, Z. Zhao, M. McDonald, J. D. Horton, J. C. Cohen, H. H. Hobbs, *J. Biol. Chem.* **2007**, *282*, 18602-18612.

[16] H. J. Kwon, T. A. Lagace, M. C. McNutt, J. D. Horton, J. Deisenhofer, *Proc. Natl. Acad. Sci. U. S. A.* **2008**, *105*, 1820-1825.

[17] P. Lo Surdo, M. J. Bottomley, A. Calzetta, E. C. Settembre, A. Cirillo, S. Pandit, Y. G. Ni, B. Hubbard, A. Sitlani, A. Carfí, *EMBO Rep.* **2011**, *12*, 1300-1305.

[18] M. S. Sabatine, R. P. Giugliano, A. C. Keech, N. Honarpour, S. D. Wiviott, S. A. Murphy, J. F. Kuder, H. Wang, T. Liu, S. M. Wasserman, P. S. Sever, T. R. Pedersen, *N. Engl. J. Med.* **2017**, *376*, 1713-1722.

[19] G. G. Schwartz, P. G. Steg, M. Szarek, D. L. Bhatt, V. A. Bittner, R. Diaz, J. M. Edelberg, S. G. Goodman, C. Hanotin, R. A. Harrington, J. W. Jukema, G. Lecorps, K. W. Mahaffey, A. Moryusef, R. Pordy, K. Quintero, M. T. Roe, W. J. Sasiela, J.-F. Tamby, P. Tricoci, H. D. White, A. M. Zeiher, *N. Engl. J. Med.* **2018**, *379*, 2097-2107.

[20] N. D. Wong, M. D. Shapiro, *Front. Cardiovasc. Med.* **2019**, *6*, 14.

[21] R. Kumar, A. Tonkin, D. Liew, E. Zomer, *Int. J. Cardiol.* **2018**, *267*, 183-187.

[22] S. Azari, A. Rezapour, N. Omidi, V. Alipour, M. Behzadifar, H. Safari, M. Tajdini, N. L. Bragazzi, *Heart Fail. Rev.* **2019**, *25*, 1077-1088.

[23] D. J. Craik, D. P. Fairlie, S. Liras, D. Price, *Chem. Biol. Drug Des.* **2013**, *81*, 136-147.

[24] M. Pelay-Gimeno, A. Glas, O. Koch, T. N. Grossmann, *Angew. Chem. Int. Ed.* **2015**, *54*, 8896-8927.

[25] Y. Zhang, L. Zhou, M. Kong-Beltran, W. Li, P. Moran, J. Wang, C. Quan, J. Tom, G. Kolumam, J. M. Elliott, N. J. Skelton, A. S. Peterson, D. Kirchhofer, *J. Mol. Biol.* **2012**, *422*, 685-696.

[26] Y. Zhang, C. Eigenbrot, L. Zhou, S. Shia, W. Li, C. Quan, J. Tom, P. Moran, P. Di Lello, N. J. Skelton, M. Kong-Beltran, A. Peterson, D. Kirchhofer, *J. Biol. Chem.* **2014**, *289*, 942-955.

[27] C. I. Schroeder, Joakim E. Swedberg, Jane M. Withka, K. J. Rosengren, M. Akcan, Daniel J. Clayton, Norelle L. Daly, O. Cheneval, Kris A. Borzilleri, M. Griffor, I. Stock, B. Colless, P. Walsh, P. Sunderland, A. Reyes, R. Dullea, M. Ammirati, S. Liu, Kim F. McClure, M. Tu, Samit K. Bhattacharya, S. Liras, David A. Price, David J. Craik, *Chem. Biol.* **2014**, *21*, 284-294.

[28] Y. Zhang, M. Ultsch, N. J. Skelton, D. J. Burdick, M. H. Beresini, W. Li, M. Kong-Beltran, A. Peterson, J. Quinn, C. Chiu, Y. Wu, S. Shia, P. Moran, P. Di Lello, C. Eigenbrot, D. Kirchhofer, *Nat. Struct. Mol. Biol.* **2017**, *24*, 848-856.

[29] D. J. Burdick, N. J. Skelton, M. Ultsch, M. H. Beresini, C. Eigenbrot, W. Li, Y. Zhang, H. Nguyen, M. Kong-Beltran, J. G. Quinn, D. Kirchhofer, *ACS Chem. Biol.* **2020**, *15*, 425-436.

[30] C. Alleyne, R. P. Amin, B. Bhatt, E. Bianchi, J. C. Blain, N. Boyer, D. Branca, M. W. Embrey, S. N. Ha, K. Jette, D. G. Johns, A. D. Kerekes, K. A. Koeplinger, D.

LaPlaca, N. Li, B. Murphy, P. Orth, A. Ricardo, S. Salowe, K. Seyb, A. Shahripour, J. R. Stringer, Y. Sun, R. Tracy, C. Wu, Y. Xiong, H. Youm, H. J. Zokian, T. J. Tucker, *J. Med. Chem.* **2020**, *63*, 13796-13824.

[31] B. J. Tombling, C. Lammi, N. Lawrence, J. Li, A. Arnoldi, D. J. Craik, C. K. Wang, *ACS Chem. Biol.* **2021**, *16*, 429-439.

[32] C. Lammi, J. Sgrignani, A. Arnoldi, G. Grazioso, *Sci. Rep.* **2019**, *9*, 2343.

[33] B. J. Tombling, C. Lammi, N. Lawrence, E. K. Gilding, G. Grazioso, D. J. Craik, C. K. Wang, *J. Med. Chem.* **2020**, *64*, 2523-2533.

[34] J. Wan, P. F. Alewood, *Angew. Chem. Int. Ed.* **2016**, *55*, 5124-5134.

[35] L. Crespo, G. Sanclimens, M. Pons, E. Giralt, M. Royo, F. Albericio, *Chem. Rev.* **2005**, *105*, 1663-1682.

[36] K. Madaan, S. Kumar, N. Poonia, V. Lather, D. Pandita, *J. Pharm. BioAllied Sci.* **2014**, *6*, 139-150.

[37] A. Santos, F. Veiga, A. Figueiras, *Materials* **2019**, *13*, 65.

[38] J. P. Tam, *Proc. Natl. Acad. Sci. U. S. A.* **1988**, *85*, 5409-5413.

[39] P. M. H. Heegaard, U. Boas, N. S. Sorensen, *Bioconjug. Chem.* **2010**, *21*, 405-418.

[40] P. Van de Vijver, M. Schmitt, D. Suylen, L. Scheer, M. C. L. G. D. Thomassen, L. J. Schurgers, J. H. Griffin, R. R. Koenen, T. M. Hackeng, *J. Am. Chem. Soc.* **2012**, *134*, 19318-19321.

[41] K. Hatano, T. Matsubara, Y. Muramatsu, M. Ezure, T. Koyama, K. Matsuoka, R. Kuriyama, H. Kori, T. Sato, *J. Med. Chem.* **2014**, *57*, 8332-8339.

[42] J. Wan, J. X. Huang, I. Vetter, M. Mobli, J. Lawson, H.-S. Tae, N. Abraham, B. Paul, M. A. Cooper, D. J. Adams, R. J. Lewis, P. F. Alewood, *J. Am. Chem. Soc.* **2015**, *137*, 3209-3212.

[43] J. Kuil, T. Buckle, J. Oldenburg, H. Yuan, A. D. Borowsky, L. Josephson, F. W. B. van Leeuwen, *Mol. Pharm.* **2011**, *8*, 2444-2453.

[44] J. Wan, M. Mobli, A. Brust, M. Muttenthaler, Å. Andersson, L. Ragnarsson, J. Castro, I. Vetter, J. X. Huang, M. Nilsson, S. M. Brierley, M. A. Cooper, R. J. Lewis, P. F. Alewood, *Aust. J. Chem.* **2017**, *70*, 162-171.

[45] H. Lu, Q. Zhou, J. He, Z. Jiang, C. Peng, R. Tong, J. Shi, *Signal Transduction Targeted Ther.* **2020**, *5*, 213.

[46] L. C. Cesa, *ChemBioChem* **2021**, *22*, 985.

[47] S. Hong, P. R. Leroueil, I. J. Majoros, B. G. Orr, J. R. Baker, M. M. Banaszak Holl, *Chem. Biol.* **2007**, *14*, 107-115.

[48] H. Li, R. Aneja, I. Chaiken, *Molecules* **2013**, *18*, 9797-9817.

[49] X. Li, M. Wang, X. Zhang, C. Liu, H. Xiang, M. Huang, Y. Ma, X. Gao, L. Jiang, X. Liu, B. Li, Y. Hou, X. Zhang, S. Yang, N. Yang, *Clin. Transl. Med.* **2020**, *9*, 16.

[50] M. Chodorge, A. J. Celeste, J. Grimsby, A. Konkar, P. Davidsson, D. Fairman, L. Jenkinson, J. Naylor, N. White, J. C. Seaman, K. Dickson, B. Kemp, J. Spooner, E. Rossy, D. C. Hornigold, J. L. Trevaskis, N. J. Bond, T. B. London, A. Buchanan, T. Vaughan, C. M. Rondinone, J. K. Osbourn, *Sci. Rep.* **2018**, *8*, 17545.

[51] M. Jain, G. Carlson, W. Cook, L. Morrow, M. Petrone, N. E. White, T. Wang, J. Naylor, P. Ambery, C. Lee, B. Hirshberg, *Diabetologia* **2019**, *62*, 373-386.

[52] X. Liu, X. Bao, M. Hu, H. Chang, M. Jiao, J. Cheng, L. Xie, Q. Huang, F. Li, C.-Y. Li, *Nature* **2020**, *588*, 693-698.

[53] A. Zorzi, S. J. Middendorp, J. Wilbs, K. Deyle, C. Heinis, *Nat. Commun.* **2017**, *8*, 16092.

[54] A. Zorzi, S. Linciano, A. Angelini, *MedChemComm* **2019**, *10*, 1068-1081.

TOC Figure

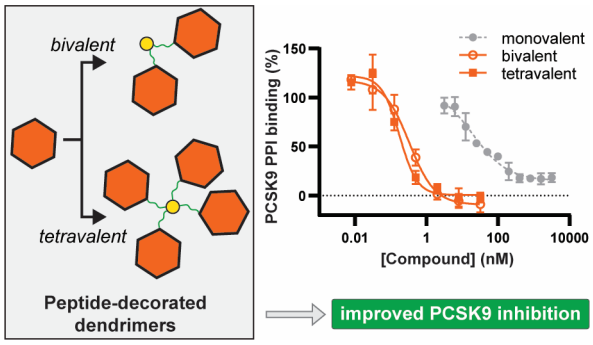

Multivalent scaffolds functionalised with PCSK9 inhibitors showed improved inhibitory activity, with the P9-38-decorated dendrimers achieving up to ~100-fold improved activity compared to monomeric P9-38. Overall, the P9-38-decorated dendrimers are a highly efficacious class of peptide-based therapeutics for targeting PCSK9 inhibition.